Using Denoisers for Accelerated CMR

Plug-and-play methods for supervised and self-supervised recovery

Rizwan Ahmad, PhD

May 5, 2022

SCMR
Society for Cardiovascular Magnetic Resonance

EACVI
European Association of Cardiovascular Imaging
European Society of Cardiology

Conflict

- No conflict to declare

Outline

- Plug-and-play (PnP) methods for CMR
- Self-calibrated PnP (ReSiDe)
- Summary

Compressed sensing (CS)

SCMR
Society for Cardiovascular Magnetic Resonance

EACVI
European Association of Cardiovascular Imaging

A pseudo-random Cartesian sampling [1,2]

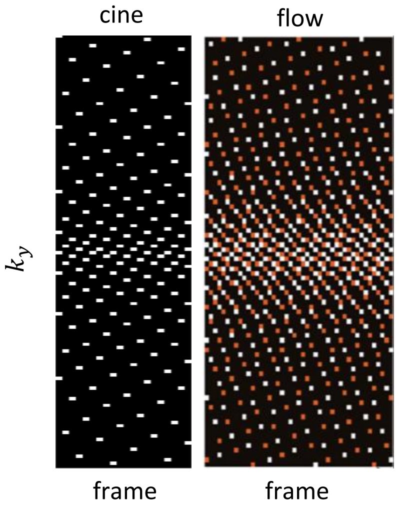

B Gadgetron-based inline reconstruction [3]

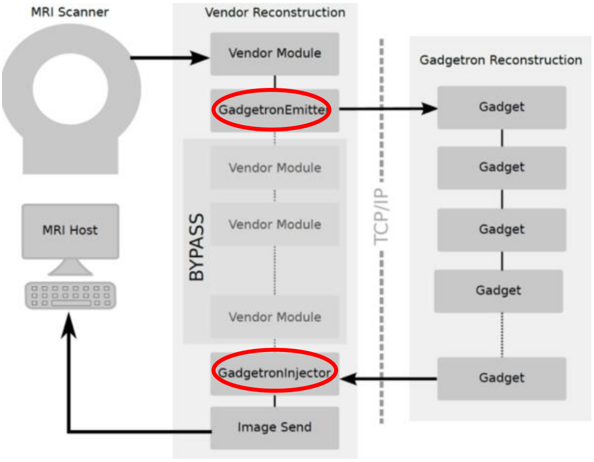

C example images from patients

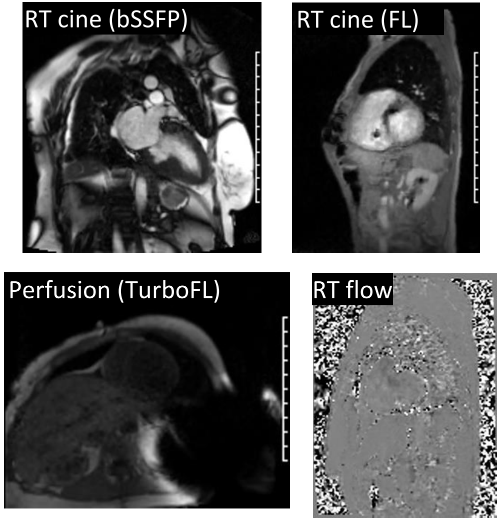

[1] Rich and Ahmad et al., MRM 2020, [2] https://github.com/OSU-CMR/GRO-CAVA, [3] http://gadgetron.github.io/, [4] Chen and Ahmad et al., MRM 2019

CMR reconstruction beyond CS [1]

- **Blind CS**
  - Lingala and Jacob, IEEE TMI, 2013
- **Low-rank approaches**
  - Zhao and Liang, IEEE TMI, 2012
  - Liu and Sun et al., MRI, 2019
- **Low-rank and sparse approaches**
  - Otazo and Sodickson et al., MRM, 2014
  - Miao and Nayak et al., MRI, 2016
- **Deep learning**
  - Küstner and Prieto et al., Scientific Reports, 2020
  - Hamilton and Seiberlich et al., MRM, 2021

[1] Bustin and Prieto et al., Front. Cardiovasc. Med. 2020

SCMR
Society for Cardiovascular Magnetic Resonance

EACVI
European Association of Cardiovascular Imaging

Plug-and-play (PnP) methods

$$\widehat{\boldsymbol{x}} = \arg\min_{\boldsymbol{x}} \{ \frac{1}{2\tau^2} \| \boldsymbol{A}\boldsymbol{x} - \boldsymbol{y} \|_2^2 + \phi(\boldsymbol{x}) \}$$

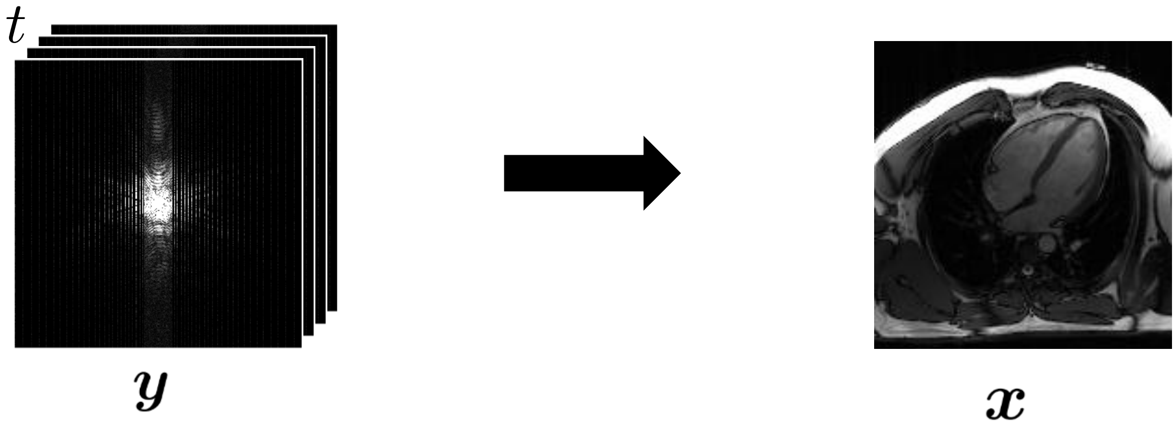

From CS to PnP

SCMR
Society for Cardiovascular Magnetic Resonance

EACVI
European Association of Cardiovascular Imaging

$$\widehat{\boldsymbol{x}} = \arg\min_{\boldsymbol{x}} \{ \frac{1}{2\tau^2} \|\boldsymbol{A}\boldsymbol{x} - \boldsymbol{y}\|_2^2 + \phi(\boldsymbol{x}) \}$$

Algorithm 1 Primal-dual splitting

Require: $\nu > 0$, τ, $\boldsymbol{A}$, $\boldsymbol{y}$

1: $\gamma = \frac{\nu}{\tau^2}\|\boldsymbol{A}\|_2^2$, $\boldsymbol{x}_0 = \boldsymbol{A}^{\mathsf{H}}\boldsymbol{y}$, $\boldsymbol{z}_0 = \boldsymbol{A}\boldsymbol{x}_0 - \boldsymbol{y}$
2: **for** $t = 1, 2, 3, \ldots$ **do**
3: $\quad \boldsymbol{u}_t = \boldsymbol{x}_{t-1} - \frac{\nu}{\tau^2}\boldsymbol{A}^{\mathsf{H}}\boldsymbol{z}_{t-1}$
4: $\quad \boldsymbol{x}_t = \arg\min_{\boldsymbol{x}} \{\phi(\boldsymbol{x}) + \frac{1}{2\nu}\|\boldsymbol{x} - \boldsymbol{u}_t\|_2^2\}$
5: $\quad \boldsymbol{v}_t = 2\boldsymbol{x}_t - \boldsymbol{x}_{t-1}$
6: $\quad \boldsymbol{z}_t = \frac{\gamma}{1+\gamma}\boldsymbol{z}_{t-1} + \frac{1}{1+\gamma}(\boldsymbol{A}\boldsymbol{v}_t - \boldsymbol{y})$
7: **end for**
8: **return** $\widehat{\boldsymbol{x}} \leftarrow \boldsymbol{x}_t$

Algorithm 2 PnP Primal-dual splitting

Require: $\nu > 0$, τ, $\boldsymbol{A}$, $\boldsymbol{y}$, $\boldsymbol{f}$

1: $\gamma = \frac{\nu}{\tau^2}\|\boldsymbol{A}\|_2^2$, $\boldsymbol{x}_0 = \boldsymbol{A}^{\mathsf{H}}\boldsymbol{y}$, $\boldsymbol{z}_0 = \boldsymbol{A}\boldsymbol{x}_0 - \boldsymbol{y}$
2: **for** $t = 1, 2, 3, \ldots$ **do**
3: $\quad \boldsymbol{u}_t = \boldsymbol{x}_{t-1} - \frac{\nu}{\tau^2}\boldsymbol{A}^{\mathsf{H}}\boldsymbol{z}_{t-1}$
4: $\quad \boldsymbol{x}_t = \boldsymbol{f}(\boldsymbol{u}_t)$
5: $\quad \boldsymbol{v}_t = 2\boldsymbol{x}_t - \boldsymbol{x}_{t-1}$
6: $\quad \boldsymbol{z}_t = \frac{\gamma}{1+\gamma}\boldsymbol{z}_{t-1} + \frac{1}{1+\gamma}(\boldsymbol{A}\boldsymbol{v}_t - \boldsymbol{y})$
7: **end for**
8: **return** $\widehat{\boldsymbol{x}} \leftarrow \boldsymbol{x}_t$

Line 4 interpretation: denoising of u_t

$f(\cdot)$: apply any denoiser

[1] Ono, IEEE Signal Process. Lett., 2017 [2] Venkatakrishnan and Wohlberg et al., IEEE GlobalSIP, 2013

PnP with application-specific denoisers

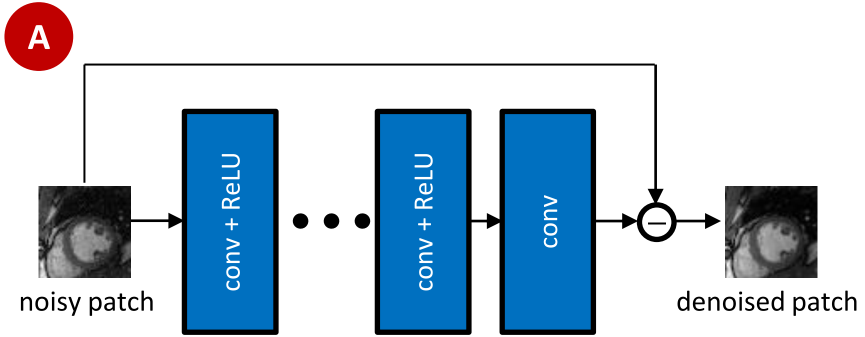

an application-specific, learned denoiser can benefit PnP [1,2]

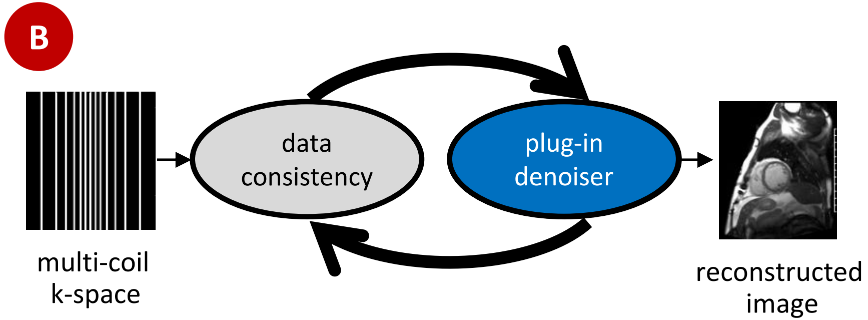

PnP methods “plug in” a denoiser into the reconstruction [3]

Training independent of the forward model

✓Highly generalizable

Physics-driven modeling

✓State-of-the-art performance

Training on image patches

✓Access to fully sampled k-space data not required

Iterative reconstruction

✗Slower than some other deep learning methods

[1] Ahmad and Schniter et al., IEEE SPM 2020, [2] Liu and Ahmad et al., IEEE ISBI 2020, [3] Venkatakrishnan et al., IEEE GlobalSIP 2013

PnP for segmented 2D cine

- Training: DL denoiser trained on 50 fully-sampled, breath-held cine images
- Validation: Nine retrospectively undersampled datasets at R = 6, 8, and 10

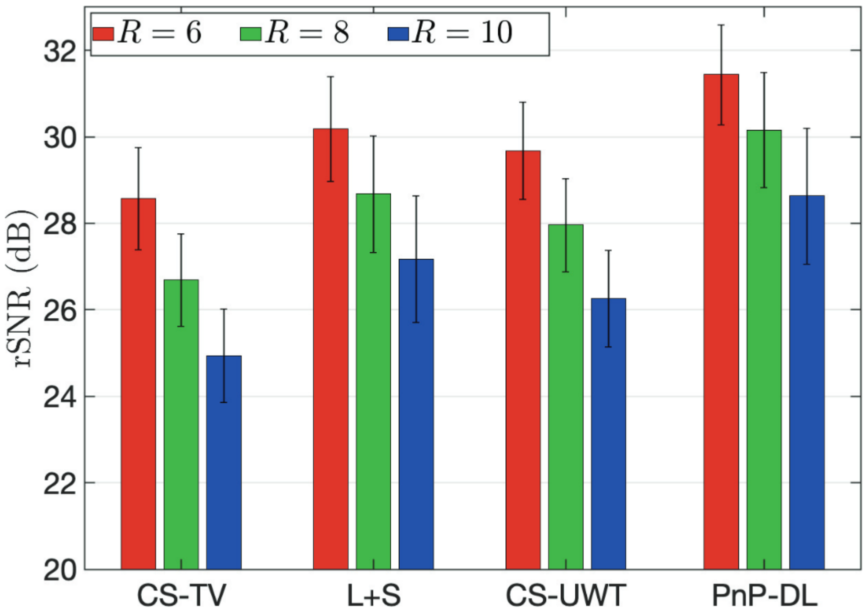

Liu and Ahmad et al., IEEE ISBI, 2020

PnP for segmented 2D cine

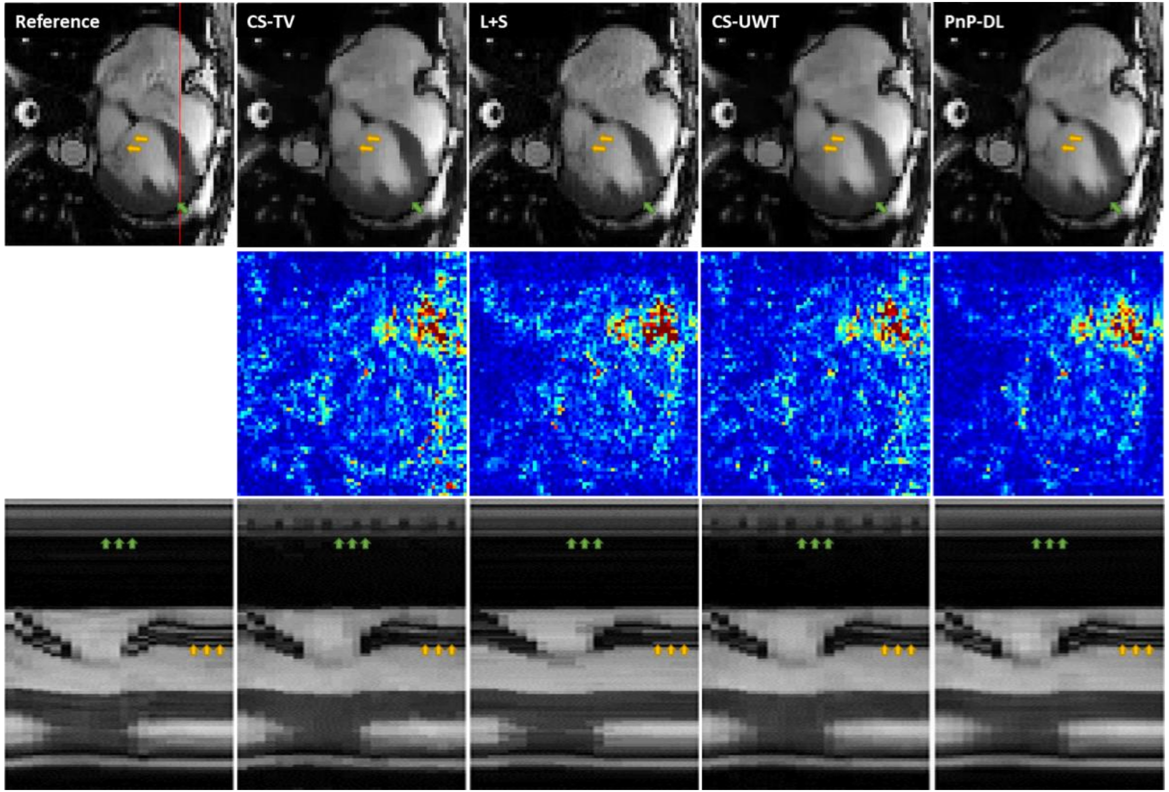

validation for the axial slice—the view not included in the training

Liu and Ahmad et al., IEEE ISBI, 2020

PnP for real-time 2D cine

- Training: DL denoiser trained on 50 fully sampled, breath-held cine images
- Validation: Ten prospectively undersampled real-time datasets scored by an expert (1—5)

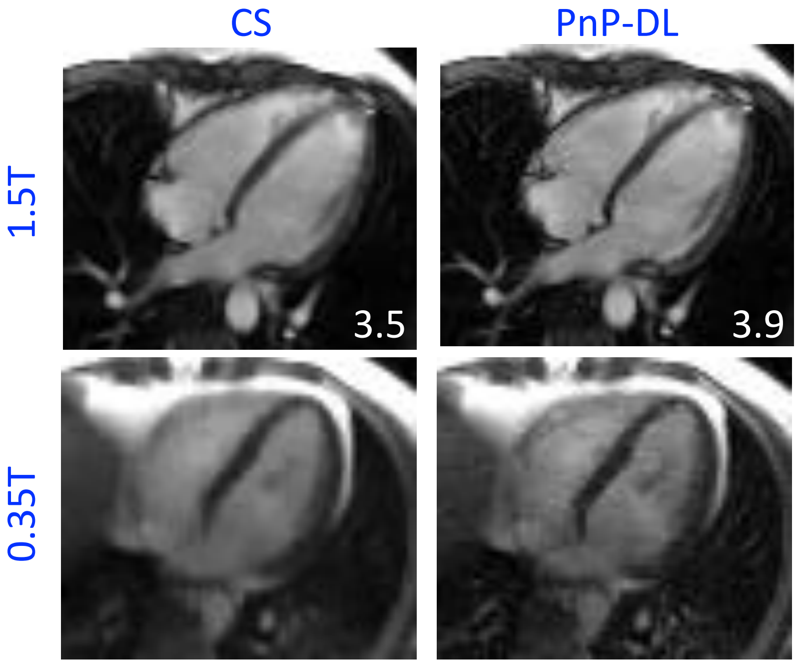

Liu and Ahmad et al., IEEE ISBI, 2020

ReSiDe: Recovery with a self-calibrated denoiser

SCMR Society for Cardiovascular Magnetic Resonance

EACVI European Association of Cardiovascular Imaging

Algorithm 2 PnP Primal-dual splitting

Require: $\nu > 0$, τ, $\boldsymbol{A}$, $\boldsymbol{y}$, $\boldsymbol{f}$

$\gamma = \frac{\nu}{\tau^2}\|\boldsymbol{A}\|_2^2$, $\boldsymbol{x}_0 = \boldsymbol{A}^{\mathsf{H}}\boldsymbol{y}$, $\boldsymbol{z}_0 = \boldsymbol{A}\boldsymbol{x}_0 - \boldsymbol{y}$
for $t = 1, 2, 3, \ldots$ **do**
    $\boldsymbol{u}_t = \boldsymbol{x}_{t-1} - \frac{\nu}{\tau^2}\boldsymbol{A}^{\mathsf{H}}\boldsymbol{z}_{t-1}$
    $\boldsymbol{x}_t = \boldsymbol{f}(\boldsymbol{u}_t)$
    $\boldsymbol{v}_t = 2\boldsymbol{x}_t - \boldsymbol{x}_{t-1}$
    $\boldsymbol{z}_t = \frac{\gamma}{1+\gamma}\boldsymbol{z}_{t-1} + \frac{1}{1+\gamma}(\boldsymbol{A}\boldsymbol{v}_t - \boldsymbol{y})$
end for
return $\widehat{\boldsymbol{x}} \leftarrow \boldsymbol{x}_t$

$\boldsymbol{f}(\cdot)$: apply any denoiser

Algorithm 3 ReSiDe

Require: $\nu > 0$, τ, $\boldsymbol{A}$, $\boldsymbol{y}$, $\boldsymbol{f}$

1: $\gamma = \frac{\nu}{\tau^2}\|\boldsymbol{A}\|_2^2$, $\boldsymbol{x}_0 = \boldsymbol{A}^{\mathsf{H}}\boldsymbol{y}$, $\boldsymbol{z}_0 = \boldsymbol{A}\boldsymbol{x}_0 - \boldsymbol{y}$
2: **for** $t = 1, 2, 3, \ldots$ **do**
3:     $\tilde{\boldsymbol{x}}_{t-1} = \boldsymbol{x}_{t-1} + \mathcal{N}(\boldsymbol{0}, \sigma_t^2\boldsymbol{I})$
4:     $\boldsymbol{\theta}_t = \mathrm{argmin}_{\boldsymbol{\theta}} \sum_{i=1}^{P} \mathcal{L}(\boldsymbol{f}(\mathcal{I}[\tilde{\boldsymbol{x}}_{t-1}]_i; \boldsymbol{\theta}), \mathcal{I}[\boldsymbol{x}_{t-1}]_i)$
5:     $\boldsymbol{u}_t = \boldsymbol{x}_{t-1} - \frac{\nu}{\tau^2}\boldsymbol{A}^{\mathsf{H}}\boldsymbol{z}_{t-1}$
6:     $\boldsymbol{x}_t = \boldsymbol{f}(\boldsymbol{u}_t; \boldsymbol{\theta}_t)$
7:     $\boldsymbol{v}_t = 2\boldsymbol{x}_t - \boldsymbol{x}_{t-1}$
8:     $\boldsymbol{z}_t = \frac{\gamma}{1+\gamma}\boldsymbol{z}_{t-1} + \frac{1}{1+\gamma}(\boldsymbol{A}\boldsymbol{v}_t - \boldsymbol{y})$
9: **end for**
10: **return** $\widehat{\boldsymbol{x}} \leftarrow \boldsymbol{x}_t$

Line 3: Add noise to x_{t-1}

Line 4: Train a denoiser to remove the added noise

$\boldsymbol{f}(\cdot\,; \boldsymbol{\theta}_t)$: apply the self-calibrated denoiser

ReSiDe—brain imaging

- Data: Multi-coil T1/T2-weighted images from fastMRI.org
- Sampling: R=2 and 4, random + ACS, pseudo-random + ACS

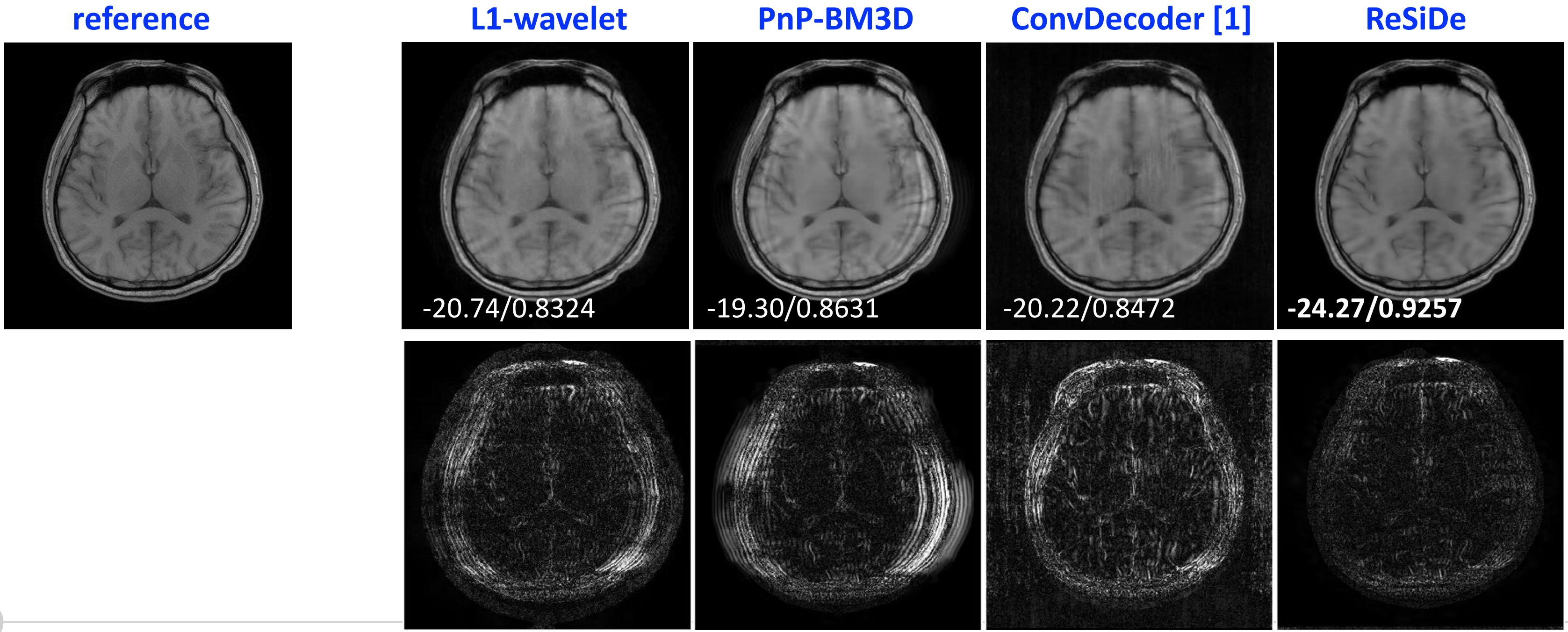

[1] Darestani and Heckel, IEEE TCI, 2021

ReSiDe—brain imaging

T1	R=2, pseudo-random	R=4, pseudo-random	R=2, random	R=4, random
L1-wavelet	-27.44 / 0.8973	-24.71 / 0.8707	-26.59 / 0.8892	-20.74 / 0.8324
PnP-BM3D	-28.60 / **0.9610**	-25.29 / **0.9361**	-27.22 / **0.9494**	-19.30 / 0.8631
ConvDecoder	-25.74 / 0.9324	-22.89 / 0.9051	-25.82 / 0.9391	-20.22 / 0.8472
ReSiDe	**-28.62** / 0.9580	**-25.97** / 0.9318	**-28.06** / 0.9491	**-24.27** / **0.9257**

T2	R=2, pseudo-random	R=4, pseudo-random	R=2, random	R=4, random
L1-wavelet	-29.52 / 0.9683	-23.83 / 0.9375	-26.78 / 0.9558	-22.09 / 0.9286
PnP-BM3D	-28.73 / 0.9573	-24.22 / **0.9414**	-27.24 / 0.9548	-23.40 / 0.9370
ConvDecoder	-24.44 / 0.9401	-20.21 / 0.9014	-24.22 / 0.9370	-19.76 / 0.8987
ReSiDe	**-30.05** / **0.9684**	**-25.18** / 0.9404	**-28.35** / **0.9654**	**-24.55** / **0.9402**

SCMR
Society for Cardiovascular Magnetic Resonance

EACVI
European Association of Cardiovascular Imaging

ReSiDe—dynamic phantom

- Data: Multi-coil MRXCAT digital phantom [1]
- Sampling: Pseudo-random Cartesian, R=8

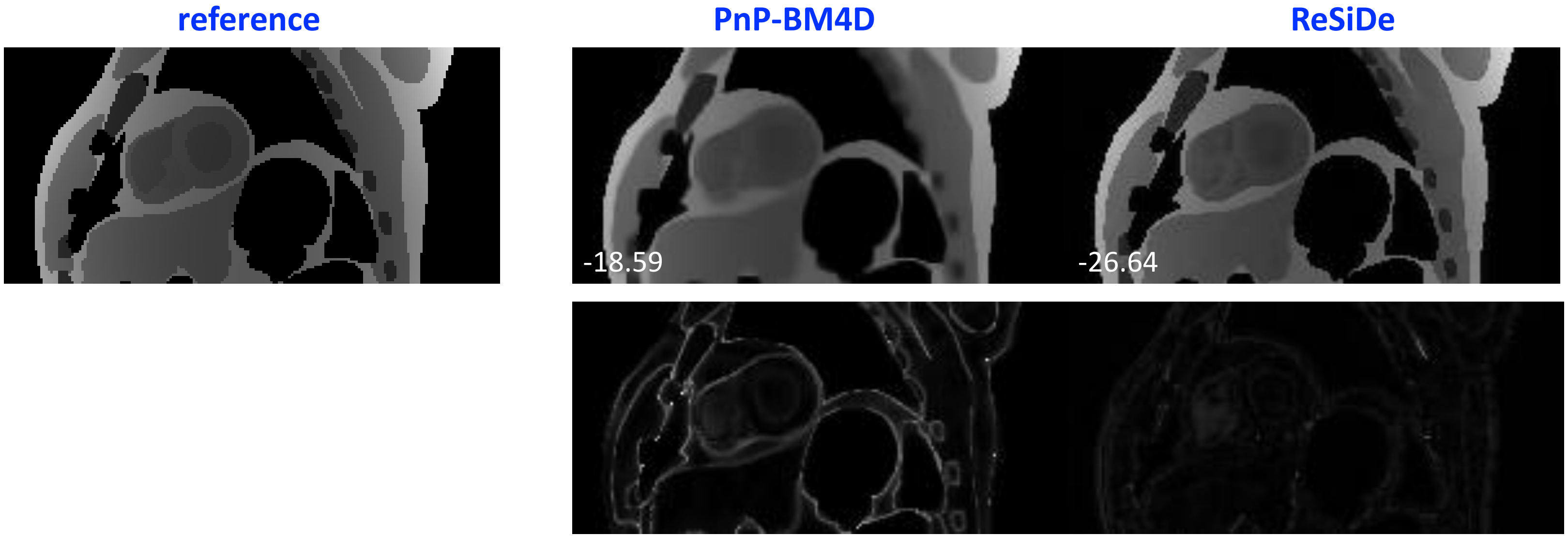

[1] Wissmann and Kozerke et al., JCMR, 2014

ReSiDe—perfusion imaging

- Data: A clinical first-pass perfusion at 1.5T
- Sampling: Rate-2 EPI

GRAPPA

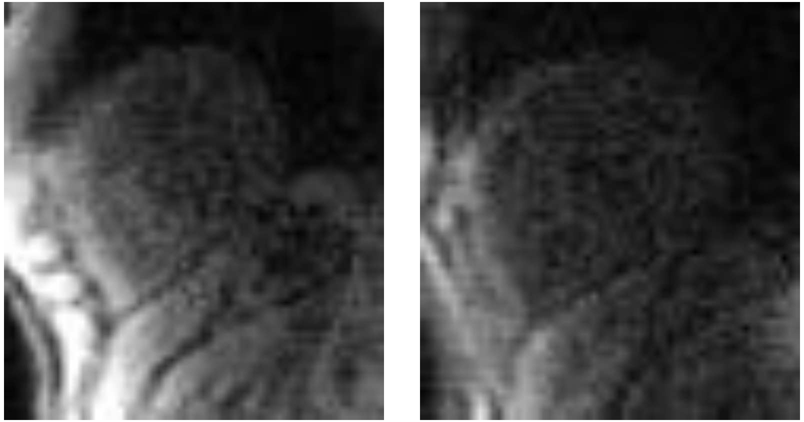

ReSiDe

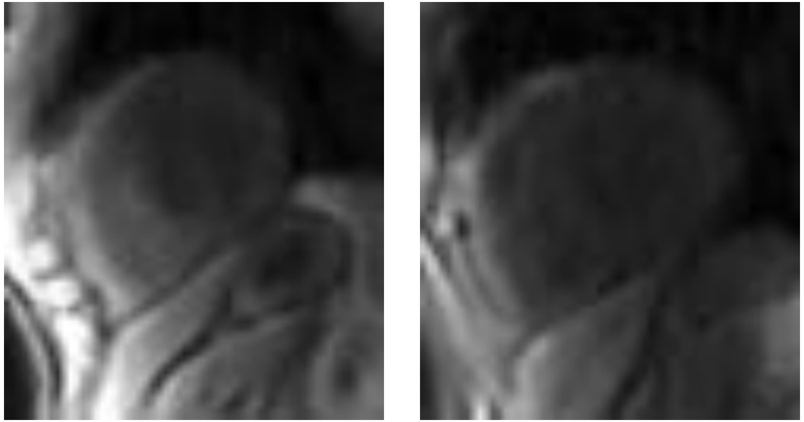

Connection of other self-calibrated methods

- **There is growing literature on training denoisers from imperfect images.**
  - Noise2Noise
    - *Lehtinen and Aila et al., arXiv, 2018*
  - Noise2Self
    - *Batson and Royer, MLR, 2019*
  - Noise2Void
    - *Krull and Jug et al., CVF, 2019*
  - Noisy-as-clean
    - *Xu and Shao et al., IEEE TIP, 2020*
  - Unsupervised learning with SURE
    - *Zhussip and Chun et al., NeurIPS, 2019*
    - *Metzler and Baraniuk et al., arXiv, 2020*
    - *Aggarwal and Jacob et al., ICASSP, 2021*

Summary

- PnP methods can leverage the power of DL by employing application-specific learned denoisers
- Many of the existing algorithms developed for CS can be used for PnP
- The denoiser can be trained on image patches
- By training the denoiser from the image that is being recovered, PnP can facilitate self-calibrated imaging

Acknowledgment

- **Collaborators**
  - Lee Potter, PhD (OSU)
  - Philip Schniter, PhD (OSU)
  - Matthew Tong, DO (OSU)
  - Karolina Zareba, MD (OSU)
  - Yuchi Han, MD (OSU)
  - Orlando Simonetti, PhD (OSU)
  - Ning Jin, PhD (Siemens)

- **Trainees/staff (OSU)**
  - Chong Chen, Yingmin Liu, Yue Pan, Debbie Scandling, Shen Zhao, Sizhuo Liu, Murtaza Arshad, Matt Bendel, Jeffrey Wen

- **Research funding**
  - National Institute of Health—NIBIB, NHLBI
  - Siemens Healthineers

SCMR Society for Cardiovascular Magnetic Resonance

EACVI European Association of Cardiovascular Imaging